Journal of Colloid and Interface Science 487 (2017) 88–96

Contents lists available at ScienceDirect

Journal of Colloid and Interface Science

journal homepage: www.elsevier.com/locate/jcis

Regular Article

Effect of solvent quality and chain density on normal and frictional forces between electrostatically anchored thermoresponsive diblock copolymer layers

Junxue An [a,*], Xiaoyan Liu [a,1], Andra Dedinaite [a,b], Evgeniya Korchagina [c], Francoise M. Winnik [c,d,e], Per M. Claesson [a,b]

[a] KTH Royal Institute of Technology, School of Chemical Science and Engineering, Department of Chemistry, Division of Surface and Corrosion Science, Drottning Kristinas väg 51, SE-100 44 Stockholm, Sweden
[b] SP Technical Research Institute of Sweden, Chemistry, Materials and Surfaces, Box 5607, SE-114 86 Stockholm, Sweden
[c] Department of Chemistry and Faculty of Pharmacy, University of Montreal, CP 6128, Succursale Centre Ville, Montreal, QC H3C3J7, Canada
[d] WPI International Center for Materials Nanoarchitectonics (MANA), National Institute for Materials Science, 1-1 Namiki, Tsukuba, Ibaraki 305-0044, Japan
[e] Department of Chemistry and Faculty of Pharmacy, University of Helsinki, Helsinki, Finland

GRAPHICAL ABSTRACT

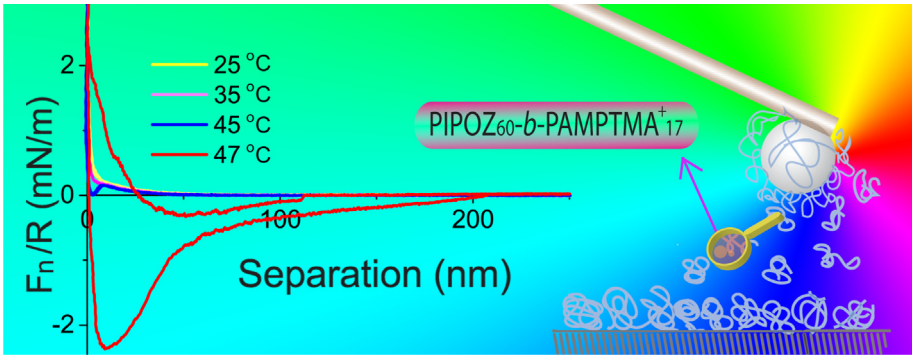

ARTICLE INFO

Article history:
Received 30 August 2016
Revised 10 October 2016
Accepted 11 October 2016
Available online 12 October 2016

Keywords:
Surface forces
Friction
Boundary lubrication
PIPOZ

ABSTRACT

Equilibration in adsorbing polymer systems can be very slow, leading to different physical properties at a given condition depending on the pathway that was used to reach this state. Here we explore this phenomenon using a diblock copolymer consisting of a cationic anchor block and a thermoresponsive block of poly(2-isopropyl-2-oxazoline), PIPOZ. We find that at a given temperature different polymer chain densities at the silica surface are achieved depending on the previous temperature history. We explore how this affects surface and friction forces between such layers using the atomic force microscope colloidal probe technique. The surface forces are purely repulsive at temperatures <40 °C. A local force minimum at short separation develops at 40 °C and a strong attraction due to capillary condensation of a polymer-rich phase is observed close to the bulk phase separation temperature. The friction forces decrease in the cooling stage due to rehydration of the PIPOZ chain. A consequence of the adsorption

* Corresponding author.
E-mail addresses: junxue@kth.se (J. An), xialiu@kemi.dtu.dk (X. Liu), andra@kth.se (A. Dedinaite), korchagina@polly.phys.msu.ru (E. Korchagina), francoise.winnik@umontreal.ca (F.M. Winnik), percl@kth.se (P.M. Claesson).
[1] Present address: Technical University of Denmark, Department of Chemistry, Kemitorvet 207, DK-2800 Kgs. Lyngby, Denmark.

http://dx.doi.org/10.1016/j.jcis.2016.10.021
0021-9797/

Poly(2-isopropyl-2-oxazoline)
Thermoresponsive polymer
Adsorption hysteresis

hysteresis is that the friction forces measured at 25 °C are significantly lower after exposure to a temperature of 40 °C than prior to heating, which is due to higher polymer chain density on the surface after heating.

1. Introduction

Many applications of temperature-responsive polymers utilize their temperature-induced conformational transition when tethered onto a solid substrate. For instance, the conformational transition can lead to changes in wetting [1], adhesion [2] and lubrication [3]. Temperature-responsive polymers that have been explored and applied to build temperature-responsive surfaces include, poly(*N*-isopropylacrylamide) (PNIPAAM) [4,5], poly(ethylene oxide) (PEO) [6] also known as poly(ethylene glycol) (PEG), poly(propylene oxide) (PPO) [7,8], methylcellulose (MC) [9] and poly(2-alkyl-2-oxazoline) [10,11]. Among these, surfaces bearing PNIPAAM chains have been widely investigated in many potential applications, like protein resistance surfaces [12], cell adhesion and detachment in cell sheet engineering [13,14] and dynamic control of gliding microtubule mobility [15]. Poly(2-oxazoline)s, discovered in 1966 [16,17], have been studied in great detail since then. In 2012, Macromolecular Rapid Communications devoted a special issue on poly(2-oxazoline)s and related pseudo-polypeptides [18]. However, these studies mainly focused on polymerization methods [19] and on the properties of poly(2-oxazolines) in bulk solution [10,11,20–24]. In recent years poly(2-oxazoline)s and derivatives have attracted increasing attention because of their promising properties in biomedical applications [25–28] and as antifouling materials [29–31].

Surfaces bearing poly(2-alkyl-2-oxazoline) chains, where the alkyl group is methyl, ethyl, or isopropyl, have been prepared by different methods, including grafting to [32,33], grafting from [31,34,35] and physisorption [29,30]. For example, the grafting to method was used by Yan et al. to covalently immobilize poly(2-ethyl-2-oxazoline) on silicon wafers and gold slides in order to form protein-resistant surfaces [31]. These films were employed in fabrication of carbohydrate microarrays and shown to reduce non-specific adsorption of lectins and, consequently, to lower the background noise [31]. Konradi et al. studied the protein-repellent properties of a poly(2-methyl-2-oxazoline) (PMOXA) based coating [30]. The polymer was electrostatically anchored to a negatively charged Nb_2O_5-coated silicon wafer via a positively charged block of poly(L-lysine). They found that the PMOXA-based coating with an optimal side-chain grafting density, approximately 10–12 monomer units per nm^2, eliminates protein adsorption as effectively as the best PEG-based coatings [30]. Our group has studied the interfacial properties of electrostatically anchored poly(2-isopropyl-2-oxazoline) (PIPOZ) layers on silica substrates, focusing particularly on the changes of the film thickness and water content within the temperature range from 25 °C to 45 °C. We observed a significant adsorption hysteresis during a heating-cooling cycle [36]. Furthermore, the interactions between such preadsorbed layers across polymer-free aqueous solutions, i.e. under conditions of temperature-independent adsorbed amount, were found to change from purely repulsive at low temperature to partly attractive at higher temperatures due to worsening of the solvent condition. The observed temperature-dependence was reproduced by mean-field modeling, which also demonstrated that the segment density profile and the degree of chain interpenetration under a given load change significantly with increasing temperature [37].

In this work, we explore how the slow equilibration affects surface and friction forces under a given condition. To this end we affect the adsorbed polymer chain density by the temperature history and utilize the atomic force microscopy (AFM) colloidal probe technique to determine surface and friction forces between $PIPOZ_{60}$-*b*-$PAMPTMA_{17}$ layers across a solution containing this polymer, covering the temperature range from 25 °C to 47 °C. Thus, unlike the previous work with pre-adsorbed layers [37], the polymer surface excess will change with temperature providing insight on how the physical properties are affected by the temperature history. Only a few reports can be found that discuss surface forces and/or friction forces between temperature-responsive surfaces under conditions that allow the surface excess to vary with temperature. These include studies of surface forces between ethyl (hydroxyethyl)cellulose (EHEC) coated hydrophilic [38] and hydrophobic surfaces [39], and electrostatically tethered PEO layers on mica surfaces [40], as well as investigations of surface and friction forces between methylcellulose (MC) coated hydrophobic surfaces [9]. Studies of this type are not only of fundamental interest, but also of high relevance for applications where products containing thermoresponsive components are exposed to varying temperatures during their storage or in processes there they are used.

2. Materials and methods

2.1. Materials

$PIPOZ_{60}$-*b*-$PAMPTMA_{17}$, see Fig. 1, with a number average molecular weight (M_n) of 10.3 kDa, was prepared as described previously [10]. The cationic PAMPTMA block, containing one charge per repeat unit, promotes the adsorption onto negatively charged silica [36]. The number of charged units per copolymer was determined to be ~17 by 1H NMR spectroscopy [10]. The non-ionic PIPOZ block (M_n = 7.0 KDa) is thermoresponsive. The phase transition temperature (cloud point) of this diblock copolymer in 0.1 mM NaCl at pH 9 with a concentration of 0.1 g/L (100 ppm) is around 49 °C (see Fig. S1). The cloud point was determined by turbidimetry measurement as described in the Supporting information. Sodium chloride (NaCl, BioXtra, ⩾99.5%) was purchased from Sigma-Aldrich and used as received. All water used was purified to a resistivity of 18.2 MΩ cm by employing a Milli-Q Purification System (Millipore, Malsheim, France) and the total organic carbon content of the water did not exceed 2 ppb.

Aqueous 0.1 mM NaCl solutions of $PIPOZ_{60}$-*b*-$PAMPTMA_{17}$ with a weight concentration of 500 ppm were prepared, and they were diluted with 0.1 mM NaCl to reach the intended concentration, 100 ppm, before use. The pH of the solutions was monitored using a pH meter (PHM 210, Meterlab) and adjusted to pH 9 by adding small amounts of HCl (0.6 M) or NaOH (1 M).

Silicon wafers (Wafer net, Germany) with a 33 nm silica layer were used as substrates and they were cut into proper size, squares with 12–14 mm sides, for the AFM experiments. The silicon wafers were cleaned by immersion in a 2% Hellmanex (Hellma GmbH) solution for 30 min, followed by rinsing with Milli-Q water excessively. They were then left in Milli-Q water overnight until

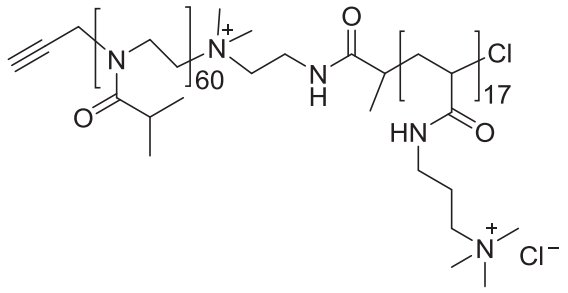

Fig. 1. Chemical structure of poly(2-isopropyl-2-oxazoline)$_{60}$-*b*-poly(3-acrylamidopropyl-trimethylammonium)$_{17}$, abbreviated as PIPOZ$_{60}$-*b*-PAMPTMA$_{17}$.

immediately before use. Prior to experiments the surfaces were rinsed with ethanol and dried with a gentle flow of filtered nitrogen gas.

2.2. Atomic force microscope (AFM) with colloidal probe

All surface forces and friction measurements were performed by using a Nanoscope Multimode 8 Pico Force AFM (Bruker, USA) in a fused silica liquid cell (volume ≈ 0.1 mL). A silica probe was attached to the end of a tipless cantilever (MikroMasch, CSC12/tipless/Cr-Au) to be used as colloidal probe. The methods of making colloidal probe and determining the normal and torsional spring constants have been described elsewhere [37].

All glassware, tubing and tools were thoroughly cleaned prior to experiments. They were immersed in 2% Hellmanex (Hellma GmbH) solution for 1 h, followed by rinsing extensively with Milli-Q water. They were then rinsed with ethanol before being dried with a stream of filtered nitrogen gas. The cantilever with silica probe was cleaned by placing it in an UV-ozone chamber with an UV intensity of 15 mW/cm^2 at a distance of one centimeter (ProCleaner™ 220, Bioforce Nanosciences, USA) for 10 min and then rinsed with Milli-Q water.

The AFM experiment was started by measuring the normal forces between silica surfaces across 0.1 mM NaCl of pH 9. Then 100 ppm PIPOZ$_{60}$-PAMPTAM$_{17}$ in 0.1 mM NaCl of pH 9 was injected into the fluid cell and the adsorption was allowed to proceed for 1 h to reach steady state. Next, normal forces were measured between the polymer layers below the phase transition temperature from 25 °C to 45 °C with 5 °C increments. Friction forces were also measured in this temperature range. In addition, surface force measurements were performed at 47 °C and 50 °C, under conditions when polymer phase separation occurs. After reaching the desired temperature 40 min were in all cases allowed before performing the force measurements.

All surface force curves were measured with a constant approach and retraction speed of 1 μm/s. The deflection sensitivity obtained for the bare silica-silica system was used to define the constant compliance and generate force curves in the presence of adsorbed polymer layers. In the friction force measurements the surfaces were first brought into contact under a given load and they were then forced to slide forwards and backwards ten times at each load. No firm evidence of stick-slip or any systematic difference between sliding cycles was noted. The scan direction was perpendicular to the cantilever, the scan length was 2 μm in one direction and the scan rate was 1 Hz, giving a sliding speed of 4 μm/s. The friction detector signal (lateral voltage) due to the twist of the cantilever was registered. The difference between the friction detector signal from the two different scanning directions for each scanning line (the first and last 20 points in each end of the scanning line corresponding to the turning of the probe on the surface were removed) were calculated, which is defined as ΔV. This quantity is then converted to friction force as described previously [41]. One friction loop is shown in the supporting information Fig. S2; and the average lateral voltage difference at one load is shown in Fig. S3, and here some further details are provided on how the reported friction force is obtained.

3. Results

We first recapitulate what is known about the adsorption properties of PIPOZ$_{60}$-*b*-PAMPTMA$_{17}$ on silica. Next, we describe how normal and friction forces between adsorbed PIPOZ$_{60}$-*b*-PAMPTMA$_{17}$ layers across 100 ppm solutions of this polymer are affected by temperature changes, bearing in mind that the temperature change also affects the adsorbed amount.

3.1. Adsorption on silica

We have previously reported how the adsorption of PIPOZ$_{60}$-*b*-PAMPTMA$_{17}$ on silica is affected by temperature and pH variations [36]. The data that are relevant for the present publication are shown in Table 1. We note that the adsorbed mass measured by ellipsometry increases significantly with increasing temperature, from 0.7 mg/m^2 at 25 °C to 1.5 mg/m^2 at 45 °C, and most of the extra adsorbed polymer chains do not desorb upon cooling. Thus, under a given temperature condition, the state of the adsorbed layer is affected by the temperature history. The number of chains per unit surface area, calculated from the surface excess, is also influenced by temperature variation. This is also shown in the Voigt mass determined by QCM-D, which includes both the mass of the adsorbed polymer and the mass of water in the layer. This quantity decreases with increasing temperature due to dehydration. The dehydration of the polymer layer leads to a slightly thinner but more compact layer, as shown by the Voigt thickness. The Voigt mass and thickness increase in the cooling step due to rehydration of the layer and the extra adsorbed polymer chains. Deposition of aggregates occurs above 45 °C [36].

We note that since the adsorbed amount is not the same at a given temperature on heating and cooling both cases cannot correspond to equilibrium. However, in both cases the system has reached a steady state since the measuring signals stabilized at each temperature (the cooling process takes about 4 h in total). Thus, we encounter long-lived trapped states that occur due to the slow polymer desorption. This is discussed in detail in our previously paper [36].

3.2. Surface forces

The forces measured between silica surfaces across a 0.1 mM NaCl (pH 9) solution are shown in Fig. 2. The long-range interaction

Table 1
Adsorption of PIPOZ$_{60}$-*b*-PAMPTMA$_{17}$ on silica from 100 ppm polymer solution in 0.1 mM NaCl at pH 9 [36]. The temperatures shown in cells with blank and italic values represent the temperature in the heating and cooling processes, respectively.

Temperature (°C)	Surface excess (mg/m^2)	Number of chains per nm^2	Voigt mass (mg/m^2)	Voigt thickness (nm)	Water content (%)
25	0.7	0.043	5.0	4.9	85
30	0.8	0.048	4.8	4.7	83
35	1.0	0.058	4.4	4.2	77
40	1.2	0.072	4.3	4.1	72
45	1.5	0.086	4.2	4.0	64
40	1.3	0.077	4.6	4.3	71
35	1.2	0.071	5.1	4.9	76
30	1.2	0.068	5.5	5.3	79
25	0.9	0.055	6.0	5.8	84

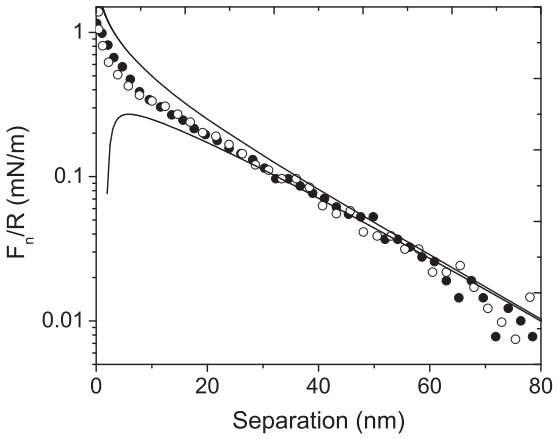

Fig. 2. Force normalized by radius as a function of separation between silica surfaces across 0.1 mM NaCl at pH 9 at 25 °C. The filled and unfilled circles represent the data collected on compression and decompression, respectively. The lines correspond to DLVO forces calculated using constant surface potential (lower line) and constant surface charge density (upper line) boundary conditions for the double layer force, respectively. A non-retarded Hamaker constant of 6.3×10^{-21} J [68] was used for calculating the van der Waals force.

is a double-layer force, and this force is characterized by a double layer potential of 39 mV and a Debye-length of 19 nm. The shorter than expected Debye-length in 0.1 mM NaCl solution (30 nm) is due to the adjustment of solution pH to 9 by addition of NaOH and HCl solutions. We note that the measured interaction falls in between that calculated assuming constant surface potential or, alternatively, constant surface charge density. Thus, as the surfaces are brought closer together the surface potential increases and the surface charge density decreases [42].

In the next step, $PIPOZ_{60}$-*b*-$PAMPTMA_{17}$ was allowed to adsorb onto the silica surface from 100 ppm solution in 0.1 mM NaCl (pH 9) for 1 h. The forces acting across the $PIPOZ_{60}$-*b*-$PAMPTMA_{17}$ polymer solution were determined at different temperatures between 25 °C and 47 °C, see Fig. 3. A double-layer force was observed at all temperatures below 47 °C. The magnitude of the double-layer potential was found to decrease slightly with increasing temperature and vary in the range of 28–21 mV, corresponding to a charge density range of 1.1–1.0 mC/m^2, which corresponds to an area per excess charge of 150–160 nm^2. The change in double-layer force is minimal compared to the increase in adsorbed mass, which increases by a factor of 2 according to Table 1. This means that the surface charge density regulates to minimize the free energy of the system as more cationic polymers adsorb to the surface, consistent with theoretical predictions [43,44].

Another important feature of the force curves presented in Fig. 3 is the temperature-dependence of the interactions observed at small separations, which are dominated by segment-segment interactions. At temperatures below 35 °C the short-range interaction is purely repulsive and no hysteresis is observed between forces measured on approach and separation. At 40 °C a notable force minimum, still on the repulsive side, is observed at a separation of about 4 nm on both approach and separation. The force minimum becomes deeper at 45 °C and a small hysteresis appears, but both approach and separation force curves remain on the repulsive side. This progressive change is due to water becoming a less good solvent for PIPOZ with increasing temperature, resulting in more favorable segment-segment interactions between and within the adsorbed layers.

The force curve changes completely as the temperature is increased to 47 °C, which is still slightly below the bulk phase transition temperature (49 °C). In this situation, the long-range force is dominated by an attraction, a deep force minimum of around 2.3 mN/m is observed on retraction and the attractive force persists to a separation of about 200 nm, showing significant hysteresis. The shape of the force curve suggests that it is due to the formation of a capillary condensate, where a polymer-rich phase is formed in the gap between the surfaces. Although bridging and depletion are two classical mechanisms leading to an attractive force between surfaces immersed in polymer solutions [45]; these two mechanisms are expected to give attractions of a shorter range than what is illustrated in Fig. 3. The capillary condensate that forms in presence of $PIPOZ_{60}$-*b*-$PAMPTMA_{17}$ in bulk solution makes the adhesion force determined in 100 ppm polymer solution about 8 times larger than that measured in absence of polymer [37].

The force between a spherical surface and a flat surface connected by a capillary condensate in the full equilibrium case, when the volume of the condensate is changing with separation to minimize the free energy, is given by Eq. (1) [46]:

$$\frac{F}{R} = 4\pi(\gamma_{sc} - \gamma_{sb})\left(1 - \frac{D}{R_k}\right) \tag{1}$$

where γ is the interfacial tension and the subscript *s*, *c* and *b* represent surface, capillary condensate and bulk, respectively. In this study, these symbols stand for silica, polymer-rich aqueous phase and polymer-dilute aqueous phase, respectively. R_k is the Kelvin radius of the capillary condensate. For the nonequilibrium situation, where the volume of the condensate is constant, Eq. (2) should be applied:

$$\frac{F}{R} = 4\pi(\gamma_{sc} - \gamma_{sb})\left(1 - \frac{1}{\sqrt{1 + \frac{R_k^2}{D^2}}}\right) \tag{2}$$

The calculated curves based on Eqs. (1) and (2) are shown in Fig. 3. An interfacial tension difference of 0.26 mN/m and a Kelvin radius of 60.5 nm were obtained as fit parameters. It is obvious that the measured force curves fall in between the full equilibrium and the constant capillary volume cases. The interfacial energy difference between the two aqueous phases with different polymer concentrations calculated here is larger than that calculated from similar surface force data in microemulsion systems, $\leqslant$0.05 mN/m [47] and smaller than that observed in a phase separated emulsion system, 3.3 mN/m [48].

3.3. Friction forces

The friction forces acting between silica surfaces coated with $PIPOZ_{60}$-*b*-$PAMPTMA_{17}$ layers at different temperatures across a 100 ppm polymer solution in 0.1 mM NaCl (pH 9) are shown in Fig. 4.

The friction forces were first measured across the 100 ppm $PIPOZ_{60}$-*b*-$PAMPTMA_{17}$ solution at 25 °C, followed by heating in 5 °C steps to 40 °C and then on cooling in steps of 5 °C down to 25 °C again. During the heating process the adsorbed amount increases significantly, whereas the decrease in adsorbed amount is less significant on cooling (see Table 1). During the cooling process, the friction force decreases with decreasing temperature (Fig. 4b) as expected from the rehydration of the PIPOZ chain, and this is similar to what has been observed for $PIPOZ_{60}$-*b*-$PAMPTMA_{17}$ coated silica surfaces across polymer-free aqueous solutions where the adsorbed amount is independent of temperature [36].

In contrast, during the initial temperature increase stage the friction forces *decreases* slightly with increasing temperature despite the worsening of the solvent condition. We suggest that this is due to the reduced interpenetration between the polymer

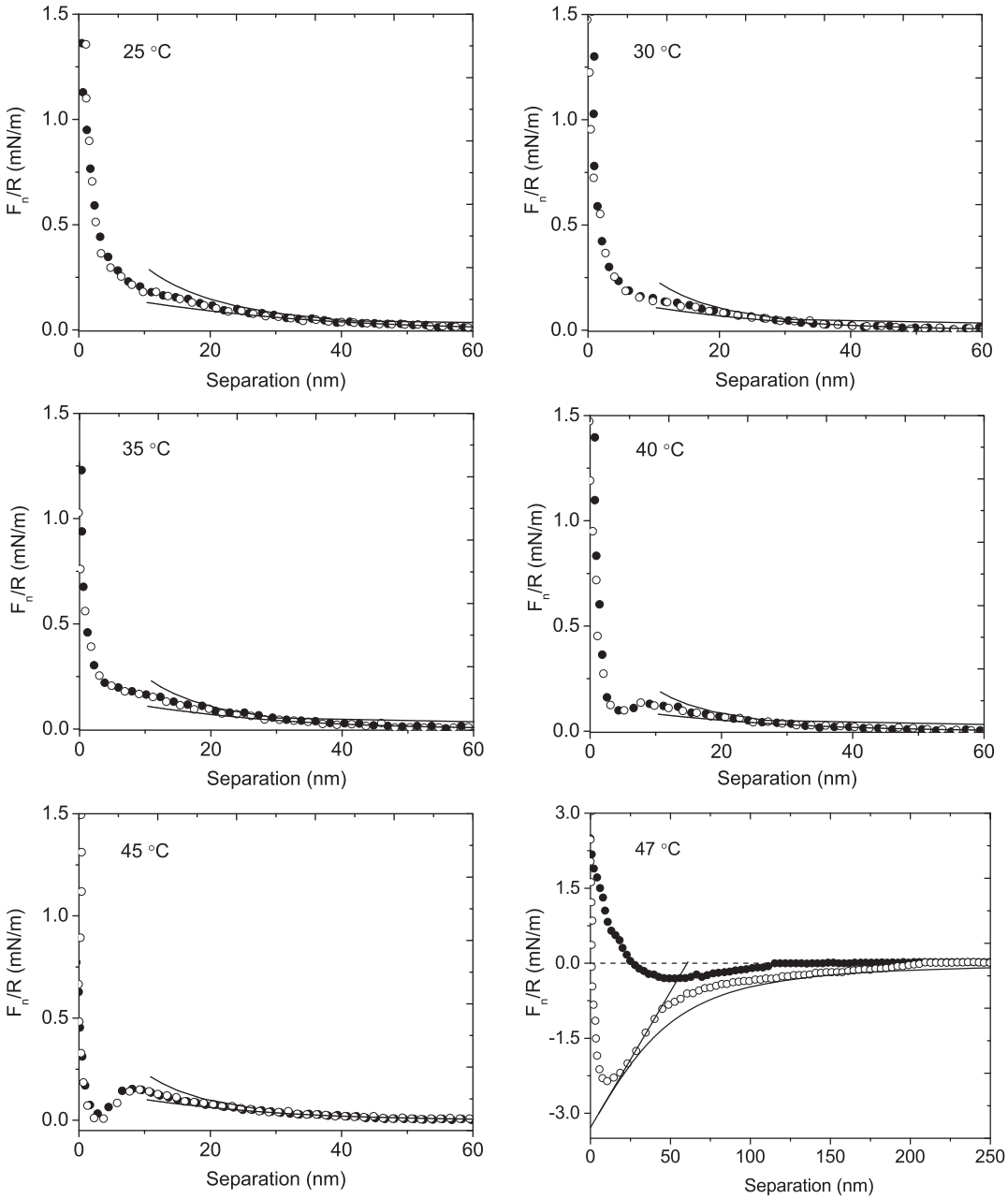

Fig. 3. Force normalized by radius as a function of separation measured on approach (filled circles) and retraction (open circles). The measurements were performed at different temperatures, as shown in the figures. The forces were measured between silica surfaces carrying adsorbed $PIPOZ_{60}$-*b*-$PAMPTMA_{17}$ layers across a 0.1 mM NaCl solution containing 100 ppm of polymer at pH 9. The upper and lower solid curves in the figures for temperatures below 47 °C are calculated double-layer forces using constant surface charge density and constant surface potential boundary conditions, respectively. The solid straight line and solid curve in the figure for 47 °C are calculated capillary forces in the full equilibrium and constant condensate volume cases, respectively.

layers resulting from the increased adsorbed amount at the higher temperature, as shown in Table 1. Consistent with this, from Fig. 4a and b we conclude that the friction force at a certain temperature on cooling is lower than that on heating as a result of the higher surface excess at the cooling stage. Clearly, the temperature history has a significant impact on friction forces.

Since the friction force is not linearly proportional to the normal load, Amontons' rule does not describe our data. Thus, we define an effective friction coefficient, μ_{eff}, as:

$$\mu_{eff} = \frac{F_f}{F_n} \tag{3}$$

where F_f and F_n are the friction force and the applied normal force (load), respectively.

The effective friction coefficient is shown as a function of load for $PIPOZ_{60}$-*b*-$PAMPTMA_{17}$ coated silica surfaces in Fig. 4c and d. First we note that when the adsorbed amount is high under good solvent conditions, i.e. at 25 °C on cooling, the effective friction coefficient is small (<0.1) up to a load of 7 nN, corresponding to a pressure of 27 MPa according to the Hertz model [49]. The peak in effective friction coefficient observed at low loads is most pronounced at high temperatures, and we attribute it to attractive interactions between the adsorbed layers during shearing. We note that the adhesion between the surfaces under shear can be significantly different to that measured during normal force measurements [50], and for surface bound chitosan gels it has been reported that the adhesion during shearing is significantly larger than that determined during normal force measurements [51].

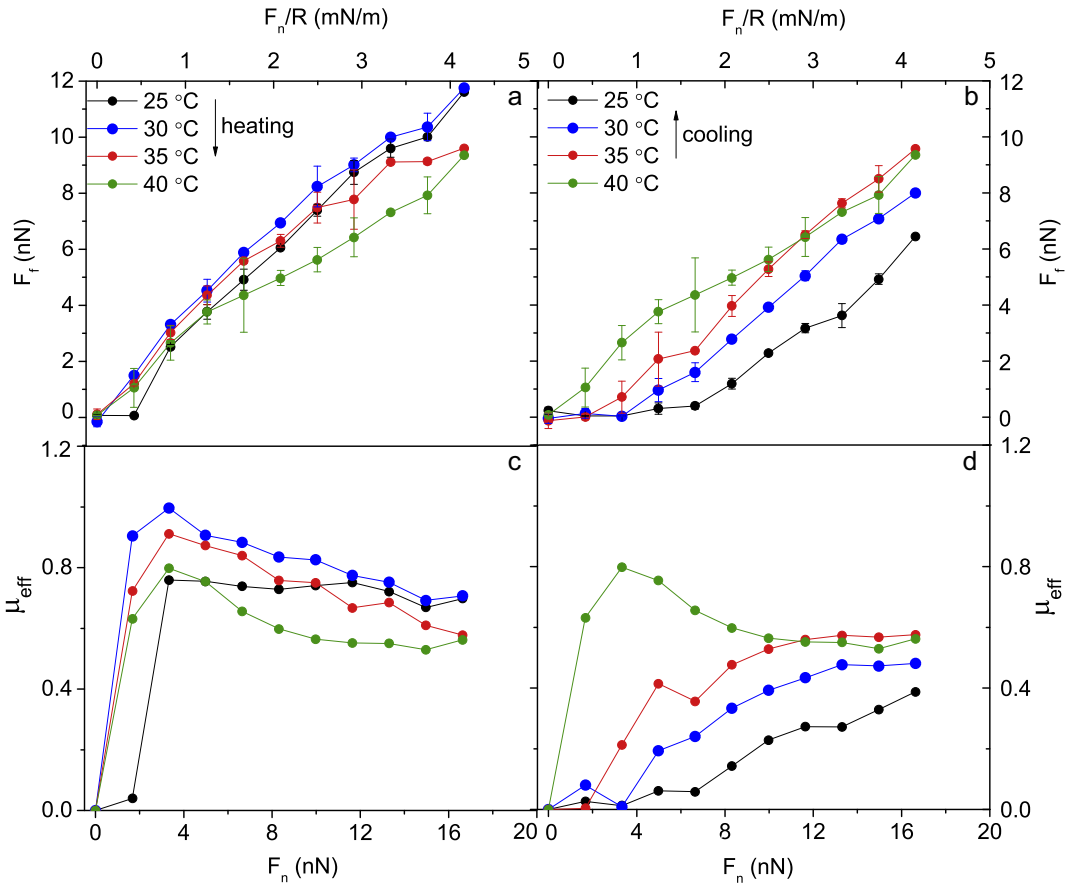

Fig. 4. Friction forces as a function of load between $PIPOZ_{60}$-*b*-$PAMPTMA_{17}$ layers measured across a 100 ppm polymer solution in 0.1 mM NaCl (pH 9) upon heating (a) and cooling (b). The effective friction coefficient corresponding to the data obtained on heating (c) and cooling (d), respectively. All figures have double x axis with upper axis labelled as F_n/R and the lower axis labelled as F_n.

Thus, we suggest that the peak in effective friction coefficient observed at low loads on heating at 30 °C and 35 °C is due to shear induced attractive interactions, even though the adhesion force measured during normal force measurements is small in these cases. Since similar peaks are not observed on cooling, when the adsorbed amount is higher, and we conclude that shear-induced attractive forces appear more readily at low adsorbed amounts.

The effective friction coefficient between $PIPOZ_{60}$-*b*-$PAMPTMA_{17}$ coated silica surfaces measured at a load of 10 nN as a function of temperature in presence and absence of polymer in bulk solution is shown in Fig. 5. In presence of $PIPOZ_{60}$-*b*-$PAMPTMA_{17}$ in bulk solution the friction coefficient increases slightly when the temperature increases from 25 °C to 30 °C as a result of dehydration of the polymer layers. It decreases continuously when the temperature increases further, which is due to the higher adsorbed amount that reduces chain interpenetration. The friction coefficient decreases in the cooling process as the adsorbed polymer layers rehydrate without too much desorption. Hence, the friction coefficients on heating are significantly higher than those on cooling at corresponding temperature.

In absence of polymer in solution, i.e. under conditions that do not allow further polymer adsorption, the friction coefficient increases with temperature due to dehydration of the polymer layers. When the temperature decreases to 25 °C, the friction coefficient also decreases due to rehydration, but it is slightly higher than the original friction coefficient determined at 25 °C before heating. This indicates that the change in the polymer layers is not fully reversible, for instance due to limited desorption of the polymer during shearing as discussed in our previous article [37].

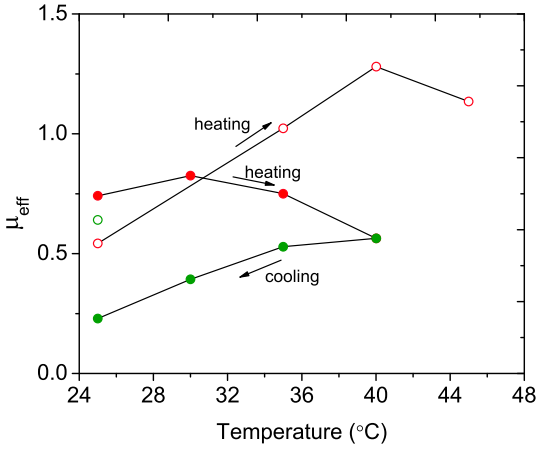

Fig. 5. The friction coefficient measured at a load of 10 nN as a function of temperature, the red and green symbols represent data obtained on heating and cooling, respectively. The filled and unfilled circles represent experiments done with and without the presence of $PIPOZ_{60}$-*b*-$PAMPTMA_{17}$ in bulk solution, respectively.

The data shown in Fig. 5 illustrates the importance of keeping track of the temperature history, and that data collected under conditions of a constant adsorbed amount even can be misleading for a situation that allows polymer adsorption to change. For instance, the increase in friction with temperature observed for the constant adsorption case is invalid when the adsorption is allowed to change with temperature, and here even a decrease in

friction with increasing temperature is observed due to the increased adsorbed amount. The reason is that both the adsorbed amount and the solvent quality influence the friction force. It decreases with increasing solvent quality and increasing adsorbed amount, resulting in a rather complex temperature-dependence when polymers are present in solution. The slow equilibration, leading to different friction forces depending on temperature history, makes the situation even more complex.

4. Discussions

4.1. Surface forces across thermoresponsive polymer solutions

The short-range interaction between surfaces coated with polymers that phase separate on heating becomes attractive (or less repulsive) at elevated temperature, as shown for polymers like ethyl(hydroxyethyl)cellulose (EHEC) [38,39], polyethylene oxide (PEO) [40,52], methylcellulose (MC) [9] and PNIPAAM [3]. The same is observed for PIPOZ$_{60}$-*b*-PAMPTMA$_{17}$ coated surfaces of this study. When the thermoresponsive polymer is present in the aqueous bulk solution, an increase in adsorbed amount is generally observed as the solvent quality is decreased [36,39,40], as also shown here. Further, a force minimum appears between PIPOZ$_{60}$-*b*-PAMPTMA$_{17}$ coated surfaces at temperatures well below the phase transition temperature, and significant attraction due to the formation of a capillary condensate is observed as the temperature is close to the phase transition temperature.

In contrast to the data presented in this work, no attractive force is observed between surfaces coated with polymers having segments that vary in hydrophobicity, such as EHEC and MC, until the temperature is several degrees above the bulk phase separation temperature. For instance, for hydrophobic surfaces coated with EHEC with a cloud point (CP) of 35 °C, across an EHEC containing aqueous solution, a very weak attraction was observed at 41 °C on separating the surfaces; and a still weak attraction was observed on both approach and separation at 52 °C [39]. Similar results were observed for hydrophobic surfaces coated with methylcellulose (MC) [9]. The observation that in case of EHEC and MC the attraction does not appear until several degrees above the cloud point can be rationalized by the fact that different segments in these polymers are not homogeneously substituted with hydrophobic groups, which results in the more hydrophobic segments being buried inside the adsorbed layer and the more hydrophilic ones being preferentially accumulated at the layer-solution interface. Thus, in these cases the onset of attraction will reflect the cloud point of the more hydrophilic segments located at the layer-solution interface.

4.2. Comparison of the temperature-response in absence and presence of polymer in bulk solution

Previously, Claesson et al. discussed the difference in interactions between EHEC coated hydrophobic surfaces in presence [39] and absence of EHEC in the bulk solution [53]. Those studies showed that the presence of polymer in solution resulted in more long-range forces at higher temperatures due to the additional adsorption that occurred as the solvent quality was decreased [39]. The attractive forces that appeared well above the cloud point were also found to be stronger in absence of polymer in bulk solution. In our study on PIPOZ$_{60}$-*b*-PAMPTMA$_{17}$ reported here we also find that the depth of the force minimum at temperatures between 35 °C and 45 °C is slightly lower in presence than in absence of polymer in the bulk solution due to the higher adsorbed amount at higher temperatures. Furthermore, the presence of polymer in bulk solution gives rise to capillary forces as the polymer solution phase separates in the gap between the surfaces slightly below the cloud point.

4.3. Capillary forces

In this work we show that strong and long-range attractive forces develop as the temperature approaches the phase transition temperature (49 °C), and we ascribed these to capillary forces caused by capillary condensation of a polymer-rich phase between the surfaces. This is consistent with our previous finding that deposition of aggregates occurred at temperature just above 45 °C [36]. Such an additional accumulation of material at the surface as the phase transition temperature is approached has also been reported for hydroxypropylmethylcellulose (HPMC) [54] and EHEC [55]. Relevant to this is a theoretical work by Linse and Wennerstrom that considers the adsorption of colloidal particles on a planar surface made of the same material using a thermodynamic chemical equilibrium model and Monte Carlo simulations [56]. The simulation results show that surface adsorption starts at a weaker particle attraction than aggregation in bulk and the equilibrium model also indicates that lateral association between particles adsorbed on the surface occurs before extensive aggregation occurs in bulk. These predictions are thus consistent with our observation that additional adsorption and capillary condensation occur just below the phase transition temperature.

Capillary forces in polymer solutions have been reported for a few other systems, such as EHEC [57,58] and mixtures of PEO and dextran [59]. In all cases, the attractive force has a region where it varies close to linearly with separation, which is typical for forces caused by capillary-induced phase separation [47]. All force curves measured in the presence of capillary condensate show large hysteresis. In our case and in the study on PEO-dextran mixtures [59], a stronger attraction is observed on separation than on approach. This is to be expected when the capillary condensate forms and grows when the two surfaces are close together. In contrast, Freyssingeas et al. observed a stronger attractive force across semidilute EHEC solutions on approach than on separation, which was ascribed to polymer being squeezed out from between the surfaces on approach [57]. We note that capillary forces in phase separating polymer systems also have been studied theoretically using lattice mean field theory [60].

4.4. Long-lived trapped states

We have shown that adsorbed amount and interactions between adsorbed PIPOZ$_{60}$-*b*-PAMPTMA$_{17}$ layers are dependent on the temperature history of the sample. Such effects are not uncommon, but seldom stressed in the scientific literature where equilibrium situations most often are in focus. However, there are some reports stressing non-equilibrium effects in mixed solutions of polymers and surfactants, where order of addition effects have been investigated and described in some detail [61–65]. The effect of trapped states on surface forces has also been noted in a few cases [66,67]. The limited scientific focus on trapped states is unfortunate since such states are common in rapid industrial processes and they also constitute a formidable challenge in formulation science. In this work we have shown significant influence of the temperature history on friction forces between adsorbed PIPOZ$_{60}$-*b*-PAMPTMA$_{17}$ layers, and rheological properties would be affected if such effects would occur in dispersions stabilized by polymers. This is a topic that clearly deserves more attention.

5. Conclusions

The surface and friction forces acting between silica surfaces across aqueous PIPOZ$_{60}$-*b*-PAMPTMA$_{17}$ solutions were investigated

as a function of temperature, with focus also on the effect of temperature history. The surface forces between the layers were found to change from a monotonically increasing repulsion with decreasing separation at 25 °C, to the appearance of a local force minimum at higher temperatures. A strong attractive force appeared due to the formation of a capillary condensate of a polymer-rich phase as the temperature approached the phase transition temperature. The friction forces were affected by both temperature and the temperature history. We find that the friction force decreases with increasing temperature despite the worsening of the solvent condition on heating; however, the opposite trend has been reported for pre-adsorbed layers where the adsorbed amount was independent of temperature [37]. Thus, results from such studies can be misleading when the adsorbed amount varies with solution condition. The reason is that the increased density of adsorbed chains at elevated temperature can counteract chain interpenetration. The importance of trapped states was also demonstrated in this study, where significantly lower friction forces were encountered on cooling than on the preceding heating stage, which is due to the higher adsorbed amount on cooling. Clearly, trapped states are of importance whenever kinetics is slow, and these can have profound effects on properties in complex formulations. For the particular case of thermoresponsive polymers, trapped states may influence the performance of products stored under varying temperature conditions.

The results demonstrate that the presence of polymer in the bulk solution during temperature variations strongly affects adhesive and frictional forces between surfaces coated with $PIPOZ_{60}$-*b*-$PAMPTMA_{17}$. The effect of the adsorption increment induced by increasing temperature on surface forces [9,38–40] and friction forces has been reported previously [9]. However, there is no previous study concerned with how the friction forces vary in a temperature cycle, and our data emphasises the importance of trapped states formed during such temperature variations. Clearly, the surface and friction forces between adsorbed PIPOZ layers in contact with an aqueous solution containing this polymer are affected by the temperature and the temperature history. This study has bearing on the application of PIPOZ in smart thermoresponsive coatings and surfaces for tissue engineering [27], where the temperature sensitivity of PIPOZ thin films are of importance as well as in the fields of nanotechnology and thermoresponsive materials, such as microfluidic channels and 'smart' coatings for control of protein adsorption.

Acknowledgement

PC and JA acknowledge financial support from the Swedish Research Council (VR). XL acknowledges a CSC scholarship grant.

Appendix A. Supplementary material

A description of turbidimetry measurement and a figure showing the measured cloud point. A figure showing one friction loop measured on trace and retrace of one scanning line and one figure showing the average lateral voltage difference of 10 scanning lines as a function of distance. This material is available free of charge via the Internet at http://pubs.acs.org. Supplementary data associated with this article can be found, in the online version, at http://dx.doi.org/10.1016/j.jcis.2016.10.021.

References

[1] P. Lenz, Wetting phenomena on structured surfaces, Adv. Mater. 11 (1999) 1531–1534.
[2] D.M. Jones, J.R. Smith, W.T.S. Huck, C. Alexander, Variable adhesion of micropatterned thermoresponsive polymer brushes: AFM investigations of poly(N-isopropylacrylamide) brushes prepared by surface-initiated polymerizations, Adv. Mater. 14 (2002) 1130–1134.
[3] A. Dedinaite, E. Thormann, G. Olanya, P.M. Claesson, B. Nystrom, A.-L. Kjoniksen, K. Zhu, Friction in aqueous media tuned by temperature-responsive polymer layers, Soft Matter 6 (2010) 2489–2498.
[4] E.S. Gil, S.M. Hudson, Stimuli-reponsive polymers and their bioconjugates, Prog. Polym. Sci. 29 (2004) 1173–1222.
[5] Z.M.O. Rzaev, S. Dinçer, E. Pişkin, Functional copolymers of N-isopropylacrylamide for bioengineering applications, Prog. Polym. Sci. 32 (2007) 534–595.
[6] P. Alexandridis, J.F. Holzwarth, Differential scanning calorimetry investigation of the effect of salts on aqueous solution properties of an amphiphilic block copolymer (poloxamer), Langmuir 13 (1997) 6074–6082.
[7] P. Alexandridis, J.F. Holzwarth, T.A. Hatton, Micellization of poly(ethylene oxide)-poly(propylene oxide)-poly(ethylene oxide) triblock copolymers in aqueous solutions: thermodynamics of copolymer association, Macromolecules 27 (1994) 2414–2425.
[8] E. Thormann, On understanding of the hofmeister effect: how addition of salt alters the stability of temperature responsive polymers in aqueous solutions, RSC Adv. 2 (2012) 8297–8305.
[9] E. Thormann, R. Bodvik, L. Karlson, P.M. Claesson, Surface forces and friction between non-polar surfaces coated by temperature-responsive methylcellulose, Colloids Surf. A 441 (2014) 701–708.
[10] E.V. Korchagina, X.-P. Qiu, F.M. Winnik, Effect of heating rate on the pathway for vesicle formation in salt-free aqueous solutions of thermosensitive cationic diblock copolymers, Macromolecules 46 (2013) 2341–2351.
[11] R. Takahashi, T. Sato, K. Terao, X.-P. Qiu, F.M. Winnik, Self-association of a thermosensitive poly(alkyl-2-oxazoline) block copolymer in aqueous solution, Macromolecules 45 (2012) 6111–6119.
[12] S. Burkert, E. Bittrich, M. Kuntzsch, M. Müller, K.-J. Eichhorn, C. Bellmann, P. Uhlmann, M. Stamm, Protein resistance of PNIPAAm brushes: application to switchable protein adsorption, Langmuir 26 (2009) 1786–1795.
[13] Y. Akiyama, A. Kikuchi, M. Yamato, T. Okano, Ultrathin poly(N-isopropylacrylamide) grafted layer on polystyrene surfaces for cell adhesion/detachment control, Langmuir 20 (2004) 5506–5511.
[14] M.A. Cooperstein, H.E. Canavan, Biological cell detachment from poly(N-isopropyl acrylamide) and its applications, Langmuir 26 (2009) 7695–7707.
[15] L. Ionov, M. Stamm, S. Diez, Reversible switching of microtubule motility using thermoresponsive polymer surfaces, Nano Lett. 6 (2006) 1982–1987.
[16] T.N.S. Kagiya, T. Maeda, K. Fukui, Ring-opening polymerization of 2-substituted 2-oxazolines, J. Polym. Sci. Part B: Polym. Lett. 4 (1966) 441–445.
[17] D.A. Tomalia, D.P. Sheetz, Homopolymerization of 2-alkyl- and 2-aryl-2-oxazolines, J. Polym. Sci. Part A-1: Polym. Chem. 4 (1966) 2253–2265.
[18] T.R. Dargaville, R. Forster, B.L. Farrugia, K. Kempe, L. Voorhaar, U.S. Schubert, R. Hoogenboom, Macromol. rapid commun. 19/2012, Macromol. Rapid Commun. 33 (2012). 1593–1593.
[19] R. Jordan, A. Ulman, Surface initiated living cationic polymerization of 2-oxazolines, J. Am. Chem. Soc. 120 (1998) 243–247.
[20] Y. Katsumoto, A. Tsuchiizu, X. Qiu, F.M. Winnik, Dissecting the mechanism of the heat-induced phase separation and crystallization of poly(2-isopropyl-2-oxazoline) in water through vibrational spectroscopy and molecular orbital calculations, Macromolecules 45 (2012) 3531–3541.
[21] J. Zhao, R. Hoogenboom, G. Van Assche, B. Van Mele, Demixing and remixing kinetics of poly(2-isopropyl-2-oxazoline) (PIPOZ) aqueous solutions studied by modulated temperature differential scanning calorimetry, Macromolecules 43 (2010) 6853–6860.
[22] C. Diehl, P. Cernoch, I. Zenke, H. Runge, R. Pitschke, J. Hartmann, B. Tiersch, H. Schlaad, Mechanistic study of the phase separation/crystallization process of poly(2-isopropyl-2-oxazoline) in hot water, Soft Matter 6 (2010) 3784–3788.
[23] T. Li, H. Tang, P. Wu, Molecular evolution of poly(2-isopropyl-2-oxazoline) aqueous solution during the liquid-liquid phase separation and phase transition process, Langmuir 31 (2015) 6870–6878.
[24] A.L. Demirel, M. Meyer, H. Schlaad, Formation of polyamide nanofibers by directional crystallization in aqueous solution, Angew. Chem. Int. Ed. 46 (2007) 8622–8624.
[25] R. Hoogenboom, Poly(2-oxazoline)s: a polymer class with numerous potential applications, Angew. Chem. Int. Ed. 48 (2009) 7978–7994.
[26] N. Oleszko, W. Wałach, A. Utrata-Wesołek, A. Kowalczuk, B. Trzebicka, A. Klama-Baryła, D. Hoff-Lenczewska, M. Kawecki, M. Lesiak, A.L. Sieroń, A. Dworak, Controlling the crystallinity of thermoresponsive poly(2-oxazoline)-based nanolayers to cell adhesion and detachment, Biomacromolecules 16 (2015) 2805–2813.
[27] V.R. de la Rosa, Poly(2-oxazoline)s as materials for biomedical applications, J. Mater. Sci.: Mater. Med. 25 (2014) 1211–1225.
[28] N. Adams, U.S. Schubert, Poly(2-oxazolines) in biological and biomedical application contexts, Adv. Drug Deliv. Rev. 59 (2007) 1504–1520.
[29] R. Konradi, B. Pidhatika, A. Muhlebach, M. Textor, Poly-2-methyl-2-oxazoline: a peptide-like polymer for protein-repellent surfaces, Langmuir 24 (2008) 613–616.
[30] R. Konradi, C. Acikgoz, M. Textor, Polyoxazolines for nonfouling surface coatings — a direct comparison to the gold standard PEG, Macromol. Rapid Commun. 33 (2012) 1663–1676.
[31] H. Wang, L. Li, Q. Tong, M. Yan, Evaluation of photochemically immobilized poly(2-ethyl-2-oxazoline) thin films as protein-resistant surfaces, ACS Appl. Mater. Interf. 3 (2011) 3463–3471.

[32] M. Agrawal, J.C. Rueda, P. Uhlmann, M. Müller, F. Simon, M. Stamm, Facile approach to grafting of poly(2-oxazoline) brushes on macroscopic surfaces and applications thereof, ACS Appl. Mater. Interf. 4 (2012) 1357–1364.
[33] F. Rehfeldt, M. Tanaka, L. Pagnoni, R. Jordan, Static and dynamic swelling of grafted poly(2-alkyl-2-oxazoline)s, Langmuir 18 (2002) 4908–4914.
[34] N. Zhang, S. Huber, A. Schulz, R. Luxenhofer, R. Jordan, Cylindrical molecular brushes of poly(2-oxazoline)s from 2-isopropenyl-2-oxazoline, Macromolecules 42 (2009) 2215–2221.
[35] N. Zhang, M. Steenackers, R. Luxenhofer, R. Jordan, Bottle-brush brushes: cylindrical molecular brushes of poly(2-oxazoline) on glassy carbon, Macromolecules 42 (2009) 5345–5351.
[36] J. An, A. Dėdinaitė, F.M. Winnik, X.-P. Qiu, P.M. Claesson, Temperature-dependent adsorption and adsorption hysteresis of a thermoresponsive diblock copolymer, Langmuir 30 (2014) 4333–4341.
[37] J. An, X. Liu, P. Linse, A. Dėdinaitė, F.M. Winnik, P.M. Claesson, Tethered poly(2-isopropyl-2-oxazoline) chains: temperature effects on layer structure and interactions probed by AFM experiments and modeling, Langmuir 31 (2015) 3039–3048.
[38] I. Pezron, E. Pezron, P.M. Claesson, M. Malmsten, Temperature-dependent forces between hydrophilic mica surfaces coated with ethyl hydroxyethyl cellulose, Langmuir 7 (1991) 2248–2252.
[39] M. Malmsten, P.M. Claesson, Temperature-dependent adsorption and surface forces in aqueous ethyl(hydroxyethyl)cellulose solutions, Langmuir 7 (1991) 988–994.
[40] P.M. Claesson, C.-G. Gölander, Direct measurements of steric interactions between mica surfaces covered with electrostatically bound low-molecular-weight polyethylene oxide, J. Colloid Interf. Sci. 117 (1987) 366–374.
[41] T. Pettersson, A. Dėdinaitė, Normal and friction forces between mucin and mucin–chitosan layers in absence and presence of SDS, J. Colloid Interf. Sci. 324 (2008) 246–256.
[42] J.N. Israelachvili, Chapter 14 – electrostatic forces between surfaces in liquids, in: J.N. Israelachvili (Ed.), Intermolecular and Surface Forces, third ed., Academic Press, San Diego, 2011, pp. 291–340.
[43] V. Shubin, P. Linse, Self-consistent-field modeling of polyelectrolyte adsorption on charge-regulating surfaces, Macromolecules 30 (1997) 5944–5952.
[44] P. Linse, P.M. Claesson, Modeling of bottle-brush polymer adsorption onto mica and silica surfaces, Macromolecules 42 (2009) 6310–6318.
[45] J.N. Israelachvili, Chapter 16 - steric (polymer-mediated) and thermal fluctuation forces, in: Intermolecular and Surface Forces, third ed., Academic Press, San Diego, 2011, pp. 381–413.
[46] D. Fennell Evans, H.W., The Colloidal Domain: Where Physics, Chemistry, Biology, and Technology Meet., 1998.
[47] P. Petrov, U. Olsson, H. Wennerström, Surface forces in bicontinuous microemulsions: water capillary condensation and lamellae formation, Langmuir 13 (1997) 3331–3337.
[48] E. Blomberg, P.M. Claesson, T. Wärnheim, Surface interactions in emulsions and liposome solutions, Colloids Surf. A 159 (1999) 149–157.
[49] K.L. Johnson, K. Kendall, A.D. Roberts, Surface energy and the contact of elastic solids, Proc. Roy. Soc. A 324 (1971) 301–313.
[50] R. Álvarez-Asencio, J. Pan, E. Thormann, M.W. Rutland, Tribological properties mapping: local variation in friction coefficient and adhesion, Tribol. Lett. 50 (2013) 387–395.
[51] C. Liu, E. Thormann, E. Tyrode, P.M. Claesson, Charge regulation and energy dissipation while compressing and sliding a cross-linked chitosan hydrogel layer, J. Colloid Interf. Sci. 443 (2015) 162–169.
[52] P.M. Claesson, R. Kjellander, P. Stenius, H.K. Christenson, Direct measurement of temperature-dependent interactions between non-ionic surfactant layers, J. Chem. Soc., Faraday Trans. 1 (82) (1986) 2735–2746.
[53] M. Malmsten, P.M. Claesson, E. Pezron, I. Pezron, Temperature-dependent forces between hydrophobic surfaces coated with ethyl hydroxyethyl cellulose, Langmuir 6 (1990) 1572–1578.
[54] R. Bodvik, L. Macakova, L. Karlson, E. Thormann, P. Claesson, Temperature-dependent competition between adsorption and aggregation of a cellulose ether—simultaneous use of optical and acoustical techniques for investigating surface properties, Langmuir 28 (2012) 9515–9525.
[55] M. Malmsten, B. Lindman, Ellipsometry studies of the adsorption of cellulose ethers, Langmuir 6 (1990) 357–364.
[56] P. Linse, H. Wennerstrom, Adsorption versus aggregation. Particles and surface of the same material, Soft Matter 8 (2012) 2486–2493.
[57] E. Freyssingeas, K. Thuresson, T. Nylander, F. Joabsson, B. Lindman, A surface force, light scattering, and osmotic pressure study of semidilute aqueous solutions of ethyl(hydroxyethyl)cellulose long-range attractive force between two polymer-coated surfaces, Langmuir 14 (1998) 5877–5889.
[58] M. Olsson, F. Joabsson, L. Piculell, Particle-induced phase separation in quasi-binary polymer solutions, Langmuir 20 (2004) 1605–1610.
[59] H. Wennerström, K. Thuresson, P. Linse, E. Freyssingeas, Long range attractive surface forces due to capillary-induced polymer incompatibility, Langmuir 14 (1998) 5664–5666.
[60] F. Joabsson, P. Linse, Capillary-induced phase separation in mixed polymer solutions. A lattice mean-field calculation study, J. Phys. Chem. B 106 (2002) 3827–3834.
[61] A. Mezei, R. Mészáros, I. Varga, T. Gilányi, Effect of mixing on the formation of complexes of hyperbranched cationic polyelectrolytes and anionic surfactants, Langmuir 23 (2007) 4237–4247.
[62] E.S. Pagac, D.C. Prieve, R.D. Tilton, Kinetics and mechanism of cationic surfactant adsorption and coadsorption with cationic polyelectrolytes at the silica–water interface, Langmuir 14 (1998) 2333–2342.
[63] K.D. Berglund, T.M. Przybycien, R.D. Tilton, Coadsorption of sodium dodecyl sulfate with hydrophobically modified nonionic cellulose polymers. 2. Role of surface selectivity in adsorption hysteresis, Langmuir 19 (2003) 2714–2721.
[64] A. Naderi, P.M. Claesson, Association between poly(vinylamine) and sodium dodecyl sulfate: effects of mixing protocol, blending procedure, and salt concentration, J. Disper. Sci. Technol. 26 (2005) 329–340.
[65] A. Naderi, P.M. Claesson, M. Bergström, A. Dėdinaitė, Trapped non-equilibrium states in aqueous solutions of oppositely charged polyelectrolytes and surfactants: effects of mixing protocol and salt concentration, Colloids Surf. A 253 (2005) 83–93.
[66] M.A.G. Dahlgren, H.C.M. Hollenberg, P.M. Claesson, The order of adding polyelectrolyte and salt affects surface forces and layer structures, Langmuir 11 (1995) 4480–4485.
[67] A. Dedinaite, P.M. Claesson, M. Bergström, Polyelectrolyte–surfactant layers: adsorption of preformed aggregates versus adsorption of surfactant to preadsorbed polyelectrolyte, Langmuir 16 (2000) 5257–5266.
[68] L. Bergström, Hamaker constants of inorganic materials, Adv. Colloid Interf. Sci. 70 (1997) 125–169.